Optics Communications 415 (2018) 146–150

Contents lists available at ScienceDirect

Optics Communications

journal homepage: www.elsevier.com/locate/optcom

Geometric effect on second harmonic generation from gold grating

Jiao Lu, Baoyong Ding, Yanyan Huo, Tingyin Ning *

School of Physics and Electronics, Shandong Provincial Key Laboratory of Optics and Photonic Device, Shandong Normal University, Jinan 250014, Shandong, China

ARTICLE INFO

Keywords:
Second harmonic generation
Surface plasmon resonance
Grating

ABSTRACT

We numerically investigate second harmonic generation from gold gratings of an ideal rectangular and ladder-shaped cross-section. The SHG efficiency from the gold gratings of the ladder-shaped cross-section is significantly enhanced compared with that from the ideal rectangular cross-section with a maximum enhancement factor of around two. The enhancement is ascribe to the nanostructure dependent local fundamental electric field, the nonlinear sources and thus the far field radiation. Our results have a practical meaning in the explanation of experimental SHG measurement, and the modulation of SHG response in the metallic nanostructure.

1. Introduction

Metallic nanostructures have distinct advantages compared with traditional dielectric materials on nonlinear optical effects. Besides the metallic nanostructure itself possesses a large nonlinear susceptibility [1], the light of resonance frequency can be highly confined around the metal to produce a strong local electromagnetic field to enhance nonlinear response [2,3]. In addition, the resonance frequency can be changed by the variation of the geometric structure, and thus the nonlinear response, that shows good tunable property for metallic nanostructures [4]. In recent years, nonlinear optical effects in diverse metallic nanostructures have been widely studied, such as second harmonic generation (SHG) [5,6], third harmonic generation (THG) [7], four-wave mixing [8] and multiphoton excited luminescence [9,10].

SHG is a nonlinear optical process of two photons combining into one photon of a double-frequency. Metal of symmetry structure brings about SHG appearing on the surface of metal and not in the metal inside [11,12]. SHG becomes a powerful tool of studying metallic nanostructures and has a wide range of practical applications. For example, the SHG images are used to detect microstructure information [13]. And it is also used in biological and chemical sensing [14].

Generally, preparations of metallic nanostructures have two ways, which are using the state-of-art nanofabrication technique and chemical growth. When we experimentally prepare samples, the emergence of geometric defects which deviate from the designed ideal structure is inevitable. The previous studies show that a minor difference between actual structure and ideal structure indeed have a great impact on the linear and nonlinear optical effects [15–18].

One dimensional grating with a periodic structure in one direction is a simple and very useful nanostructure in nano-photonics and diffractive optics. In the past, a number of studies have been done on the linear and nonlinear optical properties of gold grating [19–21]. However, the actual structure of geometric defects of the grating is not fully considered and discussed. In this paper, we numerically investigate the impact of the deviation of rectangular gold grating on linear and SHG response. Especially we focus on the gold grating of ladder-shaped cross-section, which is the most common derivation in the nanofabrication. Our results show that the geometry defects of gold grating can cause a large change in SHG response.

2. Numerical model

An equation of conduction electrons to electromagnetic field inside metal can be calculated by [21,22]

$$m_e \frac{\partial \mathbf{v}}{\partial t} + m_e(\mathbf{v}\cdot\nabla)\mathbf{v} + \mathbf{v}\gamma + e(\mathbf{E} + \mathbf{v}\times\mathbf{B}) = 0 \quad (1)$$

where m_e is the mass of conduction electrons and e the charge of electron, $\mathbf{v}$ the speed of the electronic, γ the electron collision rate, the $\mathbf{E}$ and $\mathbf{B}$ are electric field and magnetic field, respectively. Current density in the metal $\mathbf{J} = \rho\mathbf{v}$ and ρ is electric charge density. The Maxwell equation for the fundamental frequency can be written as [23]

$$\nabla\times\nabla\times\mathbf{E}^{(1)} - k_0^2\varepsilon(\omega_0)\mathbf{E}^{(1)} = 0 \quad (2)$$

where $\mathbf{E}^{(1)}$ is the electric field at fundamental frequency, k_0 is the wave vector of incident wave. $\varepsilon(\omega_0)$ is the dielectric constant under the fundamental angular frequency ω_0, $\varepsilon(\omega_0) = 1$ in the air domain, and $\varepsilon(\omega_0) = 1 - \omega_p/\left[\omega_0(\omega_0 + i\tau)\right]$ in the gold domain with ω_p and τ are the bulk plasma frequency and collision frequency of gold, respectively [24].

* Corresponding author.
E-mail address: ningtingyin@sdnu.edu.cn (T. Ning).

https://doi.org/10.1016/j.optcom.2018.01.052
Received 31 July 2017; Received in revised form 19 January 2018; Accepted 22 January 2018
0030-4018/© 2018 Elsevier B.V. All rights reserved.

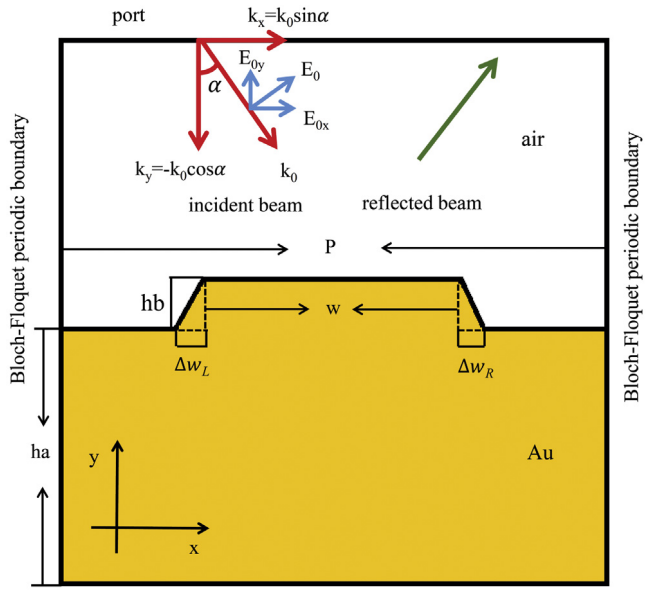

Fig. 1. The schematic diagram of cross section of periodic gold grating and setting up of our simulation. The cross section of periodic gold grating with defects Δw_L and Δw_R. P is the period of the grating, w and hb are the width and height of the gold part of grating, respectively. ha is the thickness of gold substance. The wavelength of the incident fundamental of transverse magnetic (TM) polarization is 1064 nm of the angle of incidence α, and the components of wave vector k_0 and electric field E_0 at x- and y-direction are specified. The laser intensity I_0 is around 1.67×10^6 W/m^2, or electric field $E_0 = 1.54 \times 10^4$ V/m. (For interpretation of the references to color in this figure legend, the reader is referred to the web version of this article.)

The equation for second harmonic generation under the undepleted pump approximation can be written [21]

$$\nabla \times \nabla \times \mathbf{E}^{(2)} - 4k_0^2 \epsilon(2\omega_0)\mathbf{E}^{(2)} = \frac{2i\omega_0 \tau u_0}{1 + 2i\omega_0 \tau}\mathbf{S}^{(2)} \tag{3}$$

where $\mathbf{S}^{(2)} = \frac{e}{m}(\rho^{(1)}\mathbf{E}^{(1)} + \mathbf{J}^{(1)} \times \mathbf{B}^{(1)}) + (\mathbf{J}^{(1)} \cdot \nabla)\mathbf{v}^{(1)} + \mathbf{v}^{(1)}(\nabla \cdot \mathbf{J}^{(1)})$ is the nonlinear driving force, u_0 is the vacuum permeability, $\epsilon(2\omega_0)$ is the dielectric constant at the SHG frequency.

We use the finite element method to solve the above Eqs. (2) and (3) for the linear and SHG response. The two equations are coupled by the nonlinear driving force $\mathbf{S}^{(2)}$. The steps for solving Eqs. (2) and (3) are briefly described as follows. We built one period of the grating as the simulation domain, as shown in Fig. 1. The Bloch–Floquet boundary conditions were used to describe the periodicity for fundamental and SHG wave propagation. The top and bottom boundaries of the domain were set as port boundaries. The top port in the air domain was specified as the fundamental excitation of Eq. (2). Under the angle of incidence α, the components of wave vector k_0 and electric field E_0 of transverse magnetic polarization (TM) polarization at x- and y-direction were specified, as shown in Fig. 1. The fundamental field $\mathbf{E^{(1)}}$ in the domain and the reflection were obtained by first solving Eq. (2). We then took the result of $\mathbf{E^{(1)}}$ into the $\mathbf{S^{(2)}}$ term of Eq. (3), which can be treated as the weak contribution in the finite element method. We finally got the SHG field $\mathbf{E^{(2)}}$ and the power of SHG by solving Eq. (3). In our calculation, we only emphasis on the zeroth order diffraction. In order to avoid the divergence of the numerical calculation, we set the right angle of grating into fillet of radius 5 nm. We emphasis that the fillet has no influence on our conclusions.

3. Results and discussion

The schematic diagrams of cross section of the periodic gold gratings are depicted in Fig. 1. We design the structure of a period $P = 600$ nm, gold grating of a fill factor 50% with $w = 300$ and $hb = 35$ nm, the thickness of the gold substance $ha = 200$ nm (Fig. 1). Meanwhile, we define the distance that the left side deviates from the ideal situation as Δw_L and the right side Δw_R (Fig. 1). The gratings are fabricated on the silica substrates and surrounded by the air. The light of the TM polarization is used to excite the surface plasmon resonance (SPR). The wavelength of incident fundamental light is 1064 nm and the intensity is around 1.67×10^6 W/m^2 (the corresponding electric field E_0 is around 1.54×10^4 V/m).

Table 1
The maximum values of the SHG power from the nanostructures.

Geometric structure		Maximum value of SHG (W)
$\Delta W_L = \Delta W_R = 0$		2.56×10^{-14}
$\Delta W_L = \Delta W_R \neq 0$		4.06×10^{-14}
$\Delta W_L \neq \Delta W_R$	$\Delta W_R = 0, \Delta W_L \neq 0$	3.11×10^{-14}
	$\Delta W_R \neq 0, \Delta W_L = 0$	4.71×10^{-14}
	$\Delta W_R = 5$ nm, $\Delta W_L \neq \Delta W_R$	3.19×10^{-14}
	$\Delta W_L = 5$ nm, $\Delta W_L \neq \Delta W_R$	4.28×10^{-14}

We first study the linear and SHG response from the ideal gold grating by numerical calculation. The linear optical reflection closes to zero when the angle of incidence is 49.15° (Fig. 2(a)), indicating the surface plasmon resonance (SPR) condition is satisfied. The local electric field at the SPR angle is depicted in Fig. 2(b), with the maximum enhancement factor of about 30 around the two top side corners of gold grating. The result of SHG power versus of angle of incidence is shown in Fig. 2(a), which clearly exhibits clear resonant enhancement around the angle of SPR from gold grating. We notice that the angle of SPR and the angle of maximum SHG output is not exact the same. The minor difference (0.05°) of the two angles is because the SHG output is determined not only the local fundamental field but also the diffraction efficiency at SHG wavelength of the grating. The maximum SHG conversion efficiency is around 2.5×10^{-14} at the incident laser intensity, i.e. 1.67×10^6 W/m^2. Under the light intensity 4×10^{12} W/m^2 as reported in Refs. [25,26], the SHG conversion efficiency of the gold grating is around 5.7×10^{-8}, which has the same order compared with the SHG conversion from the metallic bowtie nano-apertures, and the gold nanocups [26]. The local field distribution of generated second harmonic field around the grating at the maximum SHG output angle, along with the nonlinear driving force at x direction, Sx, and at y direction, Sy, are also plotted as in Fig. 2(c), (d) and (e), respectively.

In order to explore the influence of geometric defects on SHG response, we designedly change the values of Δw_L and Δw_R, which is corresponding to the actual nanostructures prepared by the nanofabrication technique. Next, we will study the two cases of geometric defects in detail, one is to simultaneously change the Δw_L and Δw_R, i.e. $\Delta w_L = \Delta w_R \neq 0$, and the other is asymmetrical changes, i.e. $\Delta w_L \neq \Delta w_R$.

Under the first case, we simultaneously change the $\Delta w_L = \Delta w_R = 5$, 10, 15, 20, and 25 nm, respectively. The resonant angles of reflection slightly shift to the right side with the $\Delta w_L = \Delta w_R$ increasing (not shown here). The SHG dependent on the angle of incidence from these structures is shown in Fig. 3(a). It is clear that the maximum peaks of SHG shift to the left side with the $\Delta w_L = \Delta w_R$ increasing. It also can be explained by the above statement on SHG from the ideal structure. It is also clear that the output power of SHG is increasing with the values of Δw_L and Δw_R. Comparing the SHG from the ideal structure, the maximum value of SHG from the geometry nanostructure of $\Delta w_L = \Delta w_R = 25$ nm is enhanced around twice, as shown in Table 1. In order to explain such enhancement, we further study the near-field distribution at fundamental frequency, the generated second harmonic field and the nonlinear driving force at x and y directions from the defective geometry nanostructures of $\Delta w_L = \Delta w_R = 25$ nm, respectively, as shown in Fig. 3(b) to (e). We find that the nonlinear driving force S has a significantly different distribution, including the magnitude and the phase, comparing with that in ideal grating structure. The difference

دریافت فوری ← متن کامل مقاله

ISIArticles
مرجع مقالات تخصصی ایران

✓ امکان دانلود نسخه تمام متن مقالات انگلیسی
✓ امکان دانلود نسخه ترجمه شده مقالات
✓ پذیرش سفارش ترجمه تخصصی
✓ امکان جستجو در آرشیو جامعی از صدها موضوع و هزاران مقاله
✓ امکان دانلود رایگان ۲ صفحه اول هر مقاله
✓ امکان پرداخت اینترنتی با کلیه کارت های عضو شتاب
✓ دانلود فوری مقاله پس از پرداخت آنلاین
✓ پشتیبانی کامل خرید با بهره مندی از سیستم هوشمند رهگیری سفارشات